

Contents lists available at ScienceDirect

Petroleum Science

journal homepage: www.keaipublishing.com/en/journals/petroleum-science



Original Paper

Preparation and performance evaluation of the slickwater using novel polymeric drag reducing agent with high temperature and shear resistance ability



Ming-Wei Zhao ^{a, b, *}, Zhen-Feng Ma ^{a, b}, Cai-Li Dai ^{a, b}, Wei Wu ^c, Yong-Quan Sun ^c, Xu-Guang Song ^d, Yun-Long Cheng ^e, Xiang-Yu Wang ^{a, b}

- ^a National Key Laboratory of Deep Oil and Gas, China University of Petroleum (East China), Qingdao, 266580, Shandong, China
- b Shandong Key Laboratory of Oilfield Chemistry, China University of Petroleum (East China), Qingdao, 266580, Shandong, China
- ^c Sinopec Shengli Oilfield, Dongying, 257001, Shandong, China
- ^d Department of Chemical and Materials Engineering, University of Alberta, Edmonton, AB T6G 1H9, Canada
- ^e East China Petroleum Bureau of Sinopec, Nanjing, 210011, Jiangsu, China

ARTICLE INFO

Article history: Received 30 March 2023 Received in revised form 2 November 2023 Accepted 5 November 2023 Available online 10 November 2023

Edited by Yan-Hua Sun

Keywords: Unconventional resources Polymeric drag reducing agent Slickwater High drag reduction rate Temperature resistance

ABSTRACT

Slickwater fracturing fluids are widely used in the development of unconventional oil and gas resources due to the advantages of low cost, low formation damage and high drag reduction performance. However, their performance is severely affected at high temperatures. Drag reducing agent is the key to determine the drag reducing performance of slickwater. In this work, in order to further improve the temperature resistance of slickwater, a temperature-resistant polymeric drag reducing agent (PDRA) was synthesized and used as the basis for preparing the temperature-resistant slickwater. The slickwater system was prepared with the compositions of 0.2 wt% PDRA, 0.05 wt% drainage aid nonylphenol polyoxyethylene ether phosphate (NPEP) and 0.5 wt% anti-expansion agent polyepichlorohydrindimethylamine (PDM). The drag reduction ability, rheology properties, temperature and shear resistance ability, and core damage property of slickwater were systematically studied and evaluated. In contrast to on-site drag reducing agent (DRA) and HPAM, the temperature-resistant slickwater demonstrates enhanced drag reduction efficacy at 90 °C, exhibiting superior temperature and shear resistance ability. Notably, the drag reduction retention rate for the slickwater achieved an impressive 90.52% after a 30-min shearing period. Additionally, the core damage is only 5.53%, We expect that this study can broaden the application of slickwater in high-temperature reservoirs and provide a theoretical basis for field applications.

© 2023 The Authors. Publishing services by Elsevier B.V. on behalf of KeAi Communications Co. Ltd. This is an open access article under the CC BY-NC-ND license (http://creativecommons.org/licenses/by-nc-nd/4.0/).

1. Introduction

Nowadays, the recovery of existing conventional oil and gas resources is decreasing, unconventional oil and gas resources have gained considerable attention due to their abundant reserves (Yang et al., 2022). However, unconventional oil and gas reservoirs have harsh geological conditions, such as low porosity, low permeability and no natural production capacity (Li et al., 2015; Sheng, 2017; Wu et al., 2022). Hydraulic fracturing technology is the key to increase

production of low-porosity and low-permeability reservoirs (Osiptsov, 2017), improving the oil recovery by creating complex fractures in the reservoir and high-permeability channels for oil flowing (Yang et al., 2022). Fracturing fluid plays a crucial role in hydraulic fracturing, with water-based gel, guar gum and slickwater being the most commonly used systems (Barati and Liang, 2014; Birdsell et al., 2015; Montgomery, 2013; Patel et al., 2014). Slickwater has the advantages of low cost, low formation damage and high drag reduction performance (Wang et al., 2022). Thus, it has emerged as an effective option to increase the recovery of tight reservoirs and shale gas (Guo et al., 2018; Hu et al., 2018; Wang et al., 2020a).

Slickwater with very low viscosity requires high flow rates to

^{*} Corresponding author. National Key Laboratory of Deep Oil and Gas, China University of Petroleum (East China), Qingdao, 266580, Shandong, China. *E-mail address*: zhaomingwei@upc.edu.cn (M.-W. Zhao).

deliver proppants into the reservoir (Korlepara et al., 2022; Nguyen et al., 2018). However, the high pumping discharge causes turbulence, leading to significant energy loss and increased friction in the pipeline. To overcome high frictional resistance and reduce pumping discharge, drag reducing agents with low concentration and high drag reduction efficiency are commonly used as key additives in slickwater, and have become a hot topic of research in industry and engineering (Asidin et al., 2019; Karami and Mowla, 2012; Varnaseri and Peyghambarzadeh, 2020). Polymers, mainly relying on high molecular weight to rapidly increase viscosity and form a dense spatial network through cross-linking to achieve drag reduction, have shown promise. Polyacrylamides-based polymers are favored due to their low cost, good drag reduction effect and fast viscosity-increase ability (Deng et al., 2022; Elhaei et al., 2021). However, conventional polymers are susceptible to degradation and curling under high temperature. Moreover, under turbulent flow conditions, they usually undergo vigorous mechanical shearing, resulting in poor timing of drag reduction and serious shearing degradation (Argyropoulos and Markatos, 2015). Therefore, it is urgent to synthesize a temperature-resistant polymeric drag reducing agent and develop the temperature-resistant slickwater to improve oil and gas production under high temperature conditions.

Some researchers have focused on exploring temperature-resistant polymers in recent years. Gupta and Carman (2011) developed a temperature-resistant polymer based on acrylamide monomers with sulfonic acid groups, and constructed the gel fracturing fluid with good temperature-resistance ability. Funkhouser et al. (2010) synthesized a ternary polymer based on acrylic acid (AA), acrylamide (AM) and 2-acrylamido-2-methyl-1-propanesulfonic acid (AMPS) to construct the gel fracturing fluid. Although the researchers have achieved breakthrough results in indoor experiments, there are few temperature-resistant polymers reported suitable for use as drag reducing agents in slickwater. The functional groups and structures induced by each monomer can be used to improve the temperature-resistance ability (Funkhouser et al., 2010), providing us with ideas for the synthesis of temperature-resistant drag reducing agent for slickwater.

In this work, aiming at the poor temperature-resistance ability of the conventional slickwater, the temperature-resistant slickwater was developed. Firstly, the temperature-resistant polymeric drag reducing agent (PDRA) was synthesized using the solution polymerization method. Temperature-resistant monomers with large side groups and sulfonic acid groups were optimized and copolymerized to improve the temperature resistance of polymer. Subsequently, the concentrations of PDRA, drainage aid, and antiexpansion agent were optimized. Finally, the performance of the temperature-resistant slickwater was evaluated, including drag reduction ability, rheology properties, temperature and shear resistance ability, and core damage properties.

2. Experimental

2.1. Reagents and instruments

Acrylamide (AM), 2-acrylamido-2-methyl-1-propanesulfonic acid (AMPS), acrylic acid (AA), 1-vinyl-2-pyrrolidone (NVP), (NH₄)₂S₂O₈ and NaHSO₃ were used to synthesize the polymeric drag reducing agent PDRA. Sodium dodecylbenzene sulfonate (SDSE), dodecyl trimethyl ammonium bromide (DB), sodium dodecyl sulfate (SDS), octadecyl hydroxy sulfobetaine (OHS), Triton X-100 (TX-100) and nonylphenol polyoxyethylene ether phosphate (NPEP) were used to optimize the drainage aid. KCl, NH₄Cl, polyepichlorohydrin-dimethylamine (PDM), polyepichlorohydrin-diethanolamine (PDE) and anti-expansion agent-1 (AEA1) were

used to optimize the anti-expansion agent. On-site drag reducing agent DRA and HPAM were used to comparatively evaluate the drag reduction ability and temperature and shear resistance ability. All chemicals were used as received without further purification. Deionized water and simulated formation water (2.0 wt% KCl + 5.5 wt% NaCl + 0.45 wt% MgCl $_2$ + 0.55 wt% CaCl $_2$) were prepared in the laboratory. The core sample was provided from Shengli Oilfield and had a porosity of 17.23% and permeability of 2.17 mD.

The MYP11-2A magnetic stirrer was used to mix the solutions. The Bruker FT-IR spectrometer was used to characterize the copolymer. The TX-500C full range rotary interfacial tension meter was used to measure the interfacial tension (IFT) of different systems. The JHIF-2 fracturing fluid friction tester was used to test the drag reduction performance of the drag reducing agent and temperature-resistant slickwater. The tabletop high-speed centrifuge was used to evaluate the anti-expansion rate of different systems. The HAAKE MARS 60 rheometer was used to test rheological properties. The high-pressure and high precision plunger pump as well as the TY-B core gripper were used to test the core damage rate after the temperature-resistant slickwater was used. The Sigma 300 scanning electron microscope was used to characterize the microscopic morphologies of slickwater.

2.2. The synthesis of the polymeric drag reducing agent

In this work, the temperature-resistant polymeric drag reducing agent PDRA was synthesized *via* solution polymerization method (Abdollahi et al., 2011; Chen et al., 2019; Lin et al., 2014; Pawar et al., 2016; Shi et al., 2016) as detailed in Fig. 1. The synthesis steps are summarized as follows: firstly, 8.5 g of AMPS, 26 g of AM, 0.4 g of AA, 0.1 g of NVP and 65 g of deionized water were mixed and stirred. The pH was adjusted to neutral using NaOH solution with pH meter (Sartorius PB-10). The mixture was placed in the water bath at 15 °C and nitrogen was passed in for 30 min. A certain mass fraction of compound initiator (NH₄)₂S₂O₈ and NaHSO₃ was added into the mixture (Li et al., 2013; Xu et al., 2022), and PDRA was obtained after 8 h. Fourier transform infrared (FT-IR) spectrum of PDRA was performed by KBr method.

2.3. Drag reduction test and temperature and shear resistance test

In the experimental setup, 10 L of fresh water was added to the tank, and the power pump was adjusted to ensure complete filling of the entire test pipeline with liquids. Then, the test temperature was set at 25 or 90 °C, and the heating system was initiated to maintain a stable temperature. The stable pressure difference ΔP_1 of water at the two pressure measurement points was recorded from the software. Similarly, the stable pressure difference ΔP_2 of slickwater flowing through the pipeline was measured under the same conditions and following the same procedure.

The drag reduction rate can be calculated as

$$DR = \frac{\Delta P_1 - \Delta P_2}{\Delta P_1} \times 100\% \tag{1}$$

where *DR* is the drag reduction rate of slickwater to fresh water, %. The drag reduction rate and retention rate (defined as the ratio of the drag reduction rate after a 30-min shearing period to the initial drag reduction rate) were used as the criteria for temperature and shear resistance of slickwater. The changes in the drag reduction rate were measured at a displacement of 30 L/min under different temperatures (25, 50, 75, 90 and 100 °C).

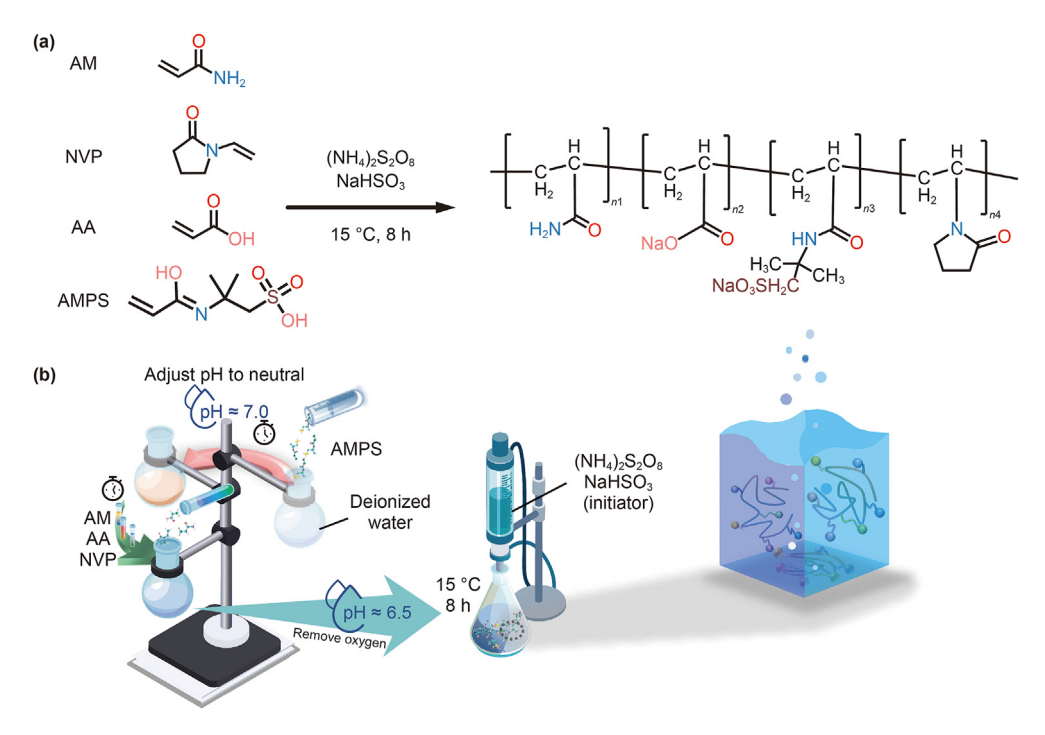


Fig. 1. Reaction structure (a) and scheme (b) of PDRA.

2.4. Anti-expansion rate test

The anti-expansion performance of various compound systems was evaluated using the centrifugal method (Wang et al., 2020b, 2021). Initially, 0.5 g of bentonite was separately added to 10 mL centrifuge tubes. Then, deionized water, kerosene and different compound systems were added and thoroughly mixed. The resulting mixture was allowed to stand at room temperature for 2 h, after which it was subjected to a tabletop high-speed centrifuge for 15 min at a rotation speed of 1500 rpm. The expansion height of bentonite in the centrifuge tubes was measured.

The anti-expansion rate can be calculated as

$$B = \frac{V_1 - V_2}{V_1 - V_3} \times 100\% \tag{2}$$

where B is anti-expansion rate, %; V_1 represents the expansion volume of bentonite in deionized water, mL; V_2 denotes the expansion volume of bentonite in the compound system, mL; and V_3 is the expansion volume of bentonite in kerosene, mL.

2.5. Rheology test

Polymers usually undergo irreversible mechanical degradation in turbulent pipes, leading to the reduction in the drag reduction effect. The viscosity of the polymer solution decreases as the shear rate increases, and this phenomenon is known as shear thinning behavior. To evaluate the viscosity of slickwater and its behavior under different shear rates, the shear viscosity of slickwater was measured at 25 °C and shear rate ranging from 0.1 to $1000 \, \mathrm{s}^{-1}$. To determine the linear viscoelastic range of the sample, stress scanning was performed. The frequency and stress of the scanning were set at 1 Hz and 1 Pa, respectively. Prior to the measurements, the sample was allowed to stabilize for at least 30 min at 25 °C.

2.6. Core damage rate test

Water-sensitive damage is a common challenge during hydraulic fracturing, and the extent to which temperature-resistant slickwater causes core damage determines its application potential. A physical simulation device (Fig. 2) was used to evaluate the core damage property of slickwater through the following experimental steps:

- (1) Core samples were cut to a diameter of 2.5 cm and a length of 5 cm. These core samples were then sonicated in deionized water for 1 h to remove residual impurities and subsequently dried in a constant temperature chamber at 90 °C for 24 h. Basic physical parameters including mass, permeability and porosity were measured, and the cores were vacuum saturated with simulated formation water.
- (2) Saturated cores were placed in the core gripper, and the initial surrounding pressure was set to 2.5 MPa. The surrounding pressure was continuously increased to 3 MPa above the pressure of injection end, and the plunger pump was turned on. The flow rate was controlled to 0.5 mL/min, and simulated formation water was injected into the core until the injection pressure stabilized. The pressure gauge was read, and the pressure difference between the two ends of the core was calculated.
- (3) The plunger pump was turned off, the core gripper was opened, and the core was removed, turned over and repositioned in the core gripper. The instrument was connected, and the plunger pump was turned on. The flow rate was controlled to 0.25 mL/min, and temperature-resistant slickwater was injected for 25–40 min, with an injection volume of 1 PV. After injection, the core gripper was placed in an oven at 90 °C for 2 h.
- (4) After heating was completed, the core gripper was cooled to room temperature, and the core was repositioned in the core

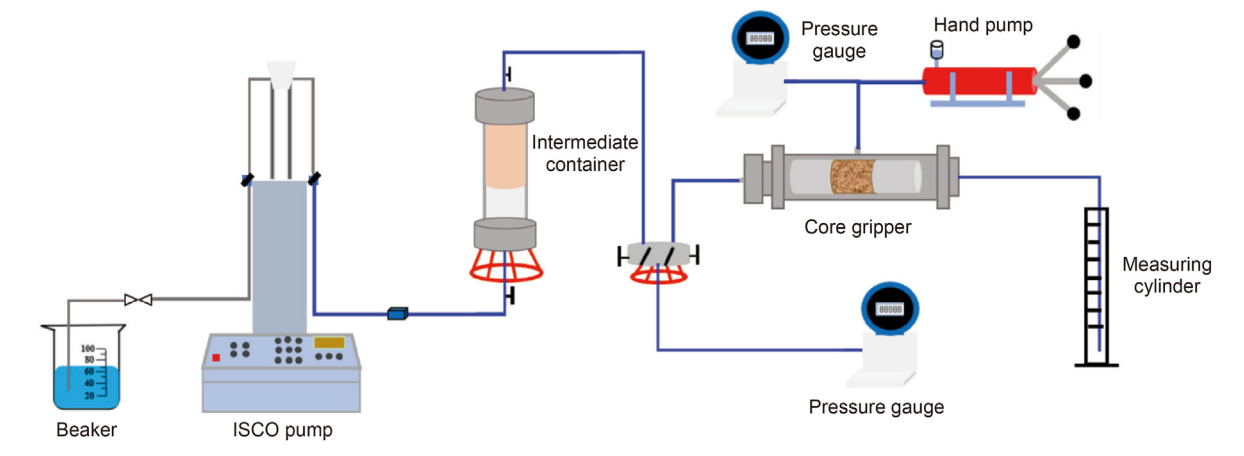


Fig. 2. Core damage evaluation device for slickwater.

gripper to its initial state. The instrument was connected, and the plunger pump was turned on, maintaining the same flow rate as the first injection. Simulated formation water was injected into the core until the injection pressure stabilized, and the pressure gauge was read. The pressure difference between the two ends of the core was calculated.

The permeability can be calculated as

$$k = 10^{-1} \frac{Q\mu L}{A\Delta p} \tag{3}$$

where k is permeability, mD; μ represents the viscosity of simulate formation water, mPa s; L denotes the core length, cm; Q is the flow rate through the core in mL/s; Δp represents the core inlet and outlet pressure difference, 10^{-3} MPa; and A denotes the core cross-sectional area, cm².

The core damage rate can be computed as

$$\eta_{\rm d} = \frac{K_0 - K_1}{K_0} \times 100\% \tag{4}$$

where η_d is the core damage rate, %; K_0 denotes the matrix permeability before slickwater entry, mD; and K_1 represents the matrix permeability upon slickwater entry, mD.

3. Results and discussion

3.1. Characterization of drag reducing agent PDRA

The copolymer PDRA was characterized by FT-IR. Multiple absorption peaks are observed in the transmittance curve of the copolymer as shown in Fig. 3. The wavenumbers corresponding to each peak are identified in the graph, and marked values are analyzed to determine the corresponding functional groups. The peak of 3342 cm⁻¹ is ascribed to the bending and contraction vibration of -NH₂, the peak of 2392 cm⁻¹ is resulted from the contraction vibration of -CH₃, the peak of 1603 cm⁻¹ is ascribed to the contraction vibration of -NH₋, and the -SO₃ peak shift to 1183 cm⁻¹. The peak of 479 cm⁻¹ is resulted from the vibration of C–S. The FT-IR spectrum confirms the effective polymerization of PDRA.

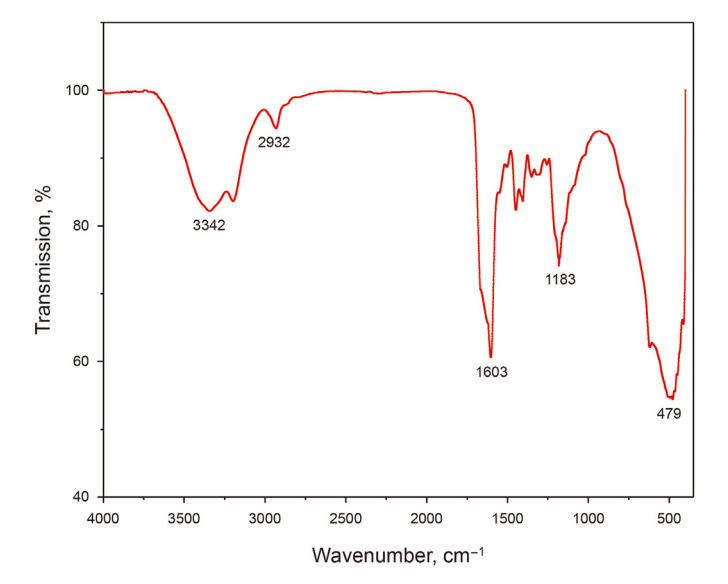


Fig. 3. FT-IR spectrum of copolymer PDRA.

3.2. Construction of temperature-resistant slickwater system

3.2.1. Concentration optimization of PDRA

The average drag reduction rates of PDRA solutions with various concentrations are presented in Fig. 4. Initially, the drag reduction rate increases with an increase in PDRA concentration. However, after reaching the concentration of 0.2 wt%, the drag reduction rate remains constant at approximately 70%. It is observed that at low concentrations, the stored elastic energy is insufficient to reduce the energy consumption of turbulent vortex. While at higher concentrations, the viscosity resistance increases, which negatively impacts the drag reduction rate (Bai et al., 2021). Hence, PDRA with a concentration of 0.2 wt% is optimized for subsequent experiments.

3.2.2. Optimization of drainage aid

The addition of drainage aid to slickwater can reduce the oil—water interfacial tension, which in turn reduces the capillary resistance during flowback. This leads to an improvement in flowback efficiency and reduction in reservoir damage. Choosing

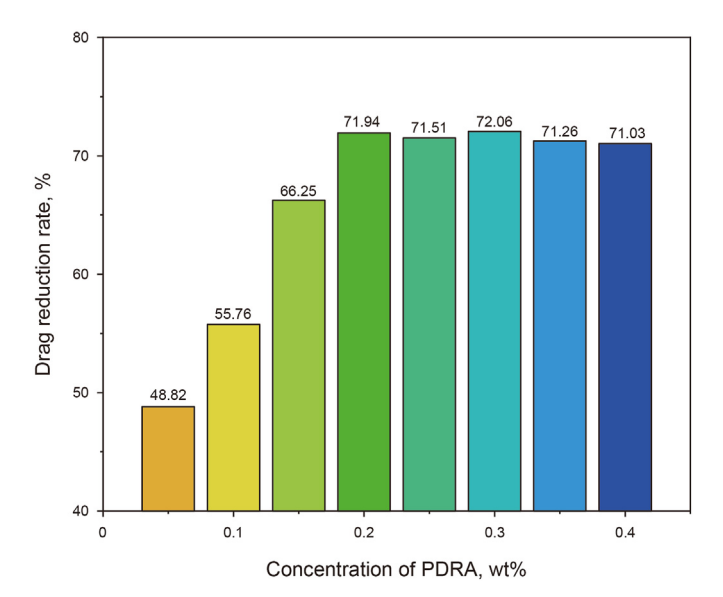


Fig. 4. Drag reduction rates of PDRA solutions at different concentrations.

the suitable drainage aid is crucial to ensure compatibility with the slickwater and temperature resistance. Long-chain cationic surfactants were found to decrease the stability of the slickwater. SDSE, SDS, DB, OHS, TX-100 and NPEP were initially selected for interfacial tension test. The results, as shown in Fig. 5(a), indicate that the interfacial tension of the compound system significantly decreases with increasing concentration of the drainage aid. Three drainage aids, OHS, TX-100 and NPEP, were selected for further evaluation of temperature resistance according to industry standards, with a preferred standard of 2 mN/m.

The drag reduction rates of 0.2 wt% PDRA and different drainage aid compound systems were evaluated at 90 °C and 30 L/min under continuous shearing. As shown in Fig. 5(b), NPEP exhibited effective improvement in the temperature resistance of the system. The hydrogen bonds formed between the oxygen atoms in NPEP and the hydrogen atoms in the polymer molecule enhanced the strength of the spatial network structure formed by the hydrophobic association of polymer. In contrast, the other two systems showed significantly lower drag reduction rates than the PDRA solution. This can be attributed to their lack of stabilizing effect on the polymer structure, which adversely affected the spatial

network structure of the polymer at high displacement, resulting in a lower drag reduction effect. Based on the comprehensive considerations of cost, interfacial activity and temperature resistance, a mass concentration of 0.05 wt% NPEP is recommended as the optimized drainage aid for slickwater.

3.2.3. Optimization of anti-expansion agent

Formation damage caused by the hydration swelling and dispersion transport of clay minerals can greatly reduce the productivity of reservoirs during slickwater fracturing. Therefore, it is crucial to develop slickwater with good anti-expansion properties. The anti-expansion performance of PDRA and different anti-expansion agent compound systems was evaluated as shown in Fig. 6(a). The results indicate that the anti-expansion rate increases with the concentration of the anti-expansion agent. Specifically, the anti-expansion rate of 2 wt% KCl, 1 wt% NH₄Cl and 0.5 wt% PDM can reach more than 90%. Based on these results, these three anti-expansion agents were selected for further temperature resistance evaluation.

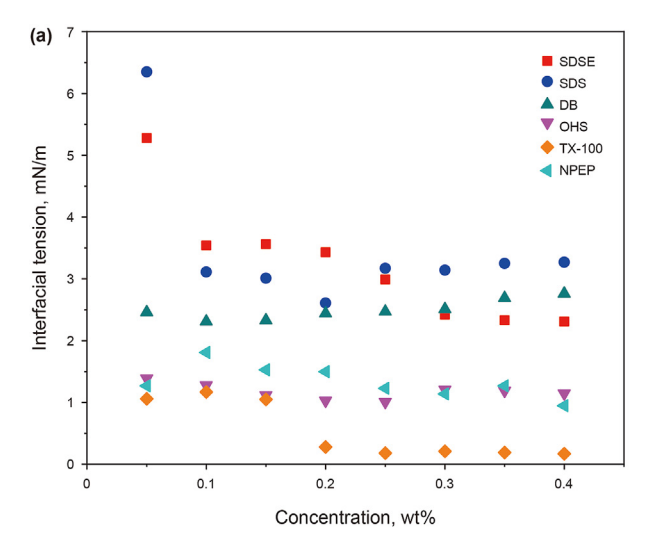
The drag reduction rates of 0.2 wt% PDRA, along with various anti-expansion agent compound systems, were experimentally evaluated under continuous shearing at 90 °C and 30 L/min. The drag reduction effects of four systems at a fixed displacement are depicted in Fig. 6(b). Notably, the drag reduction rate of PDRA and PDM complex system is slightly superior to the pure drag reducing agent system. Furthermore, the highest drag reduction rate of 72.09% is due to the mutual cross-linking of polymers, which strengthens the stability of the mesh structure. Taking into account the cost, anti-expansion rate and temperature resistance effect, PDM with a mass concentration of 0.5 wt% is the optimized anti-expansion agent of slickwater.

In summary, based on the experimental outcomes, the optimized formulation of the temperature-resistant slickwater system comprises 0.2 wt% drag reducing agent PDRA, 0.05 wt% drainage aid NPEP and 0.5 wt% anti-expansion agent PDM.

3.3. Performance evaluation of the temperature-resistant slickwater

3.3.1. Drag reduction ability

The drag reducing effects of temperature-resistant slickwater, commercially available drag reducing agent DRA and HPAM were evaluated under variable displacement. Fig. 7 shows that at room temperature, drag reducing agent DRA exhibits the best drag



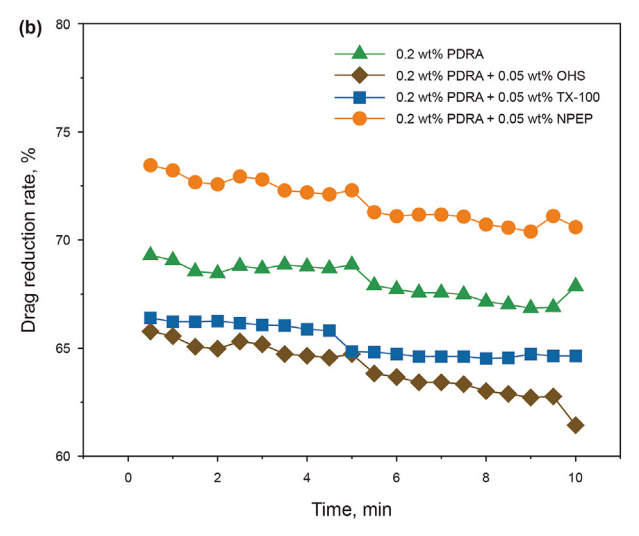


Fig. 5. (a) Oil—water interfacial tension of PDRA and different drainage aid compound systems. (b) Drag reducing effects of different compound systems.

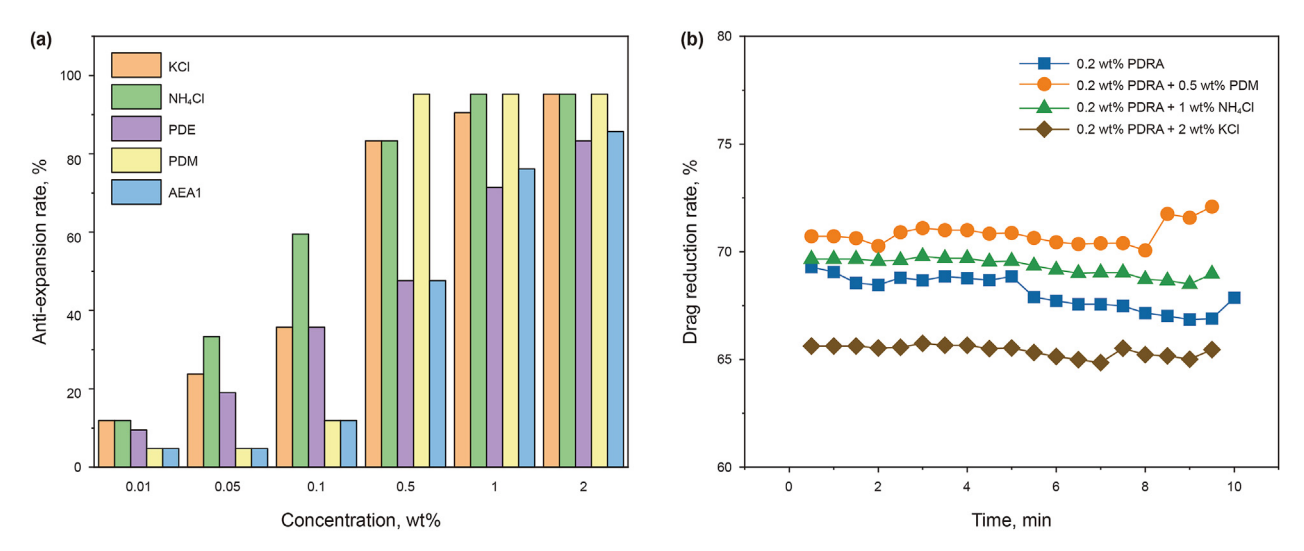


Fig. 6. (a) Anti-expansion rates of PDRA and different anti-expansion agent compound systems. (b) Drag reducing effects of different compound systems.

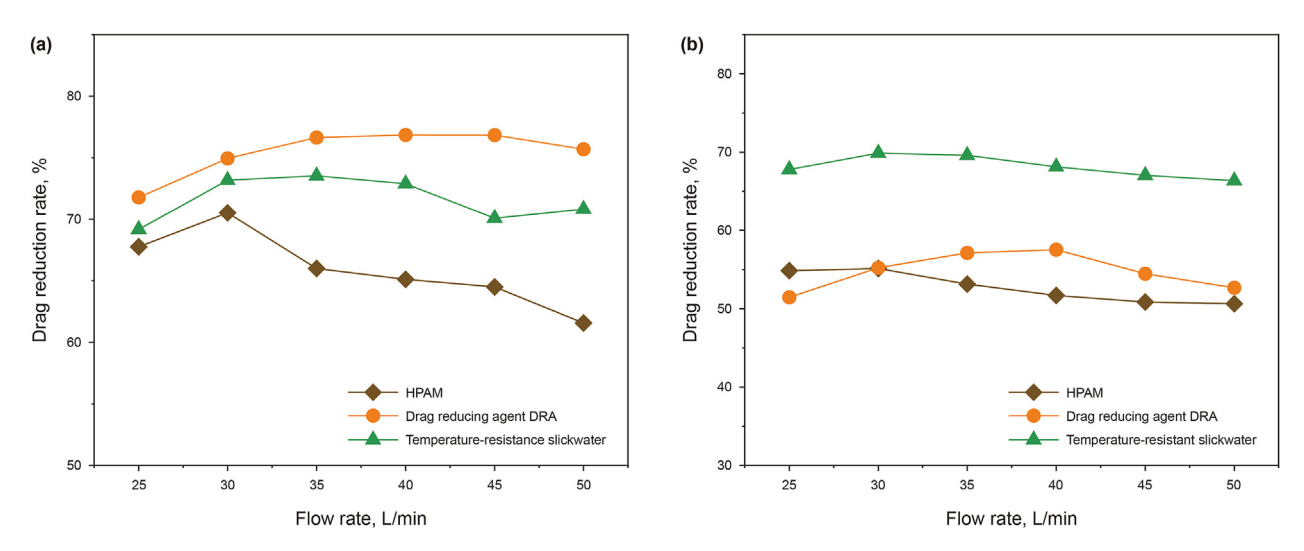
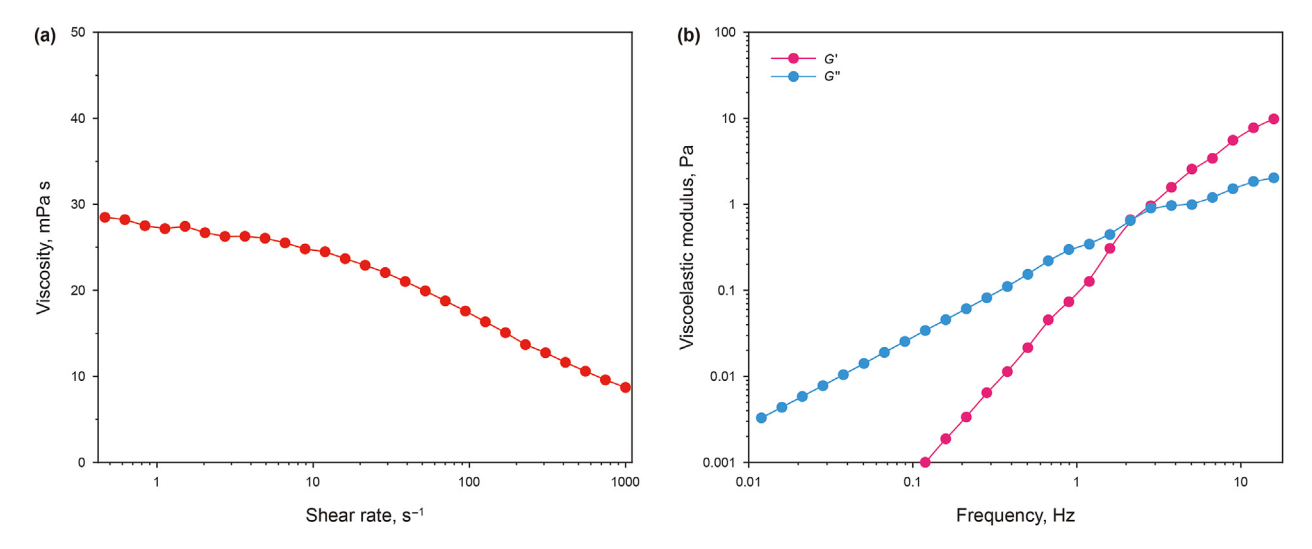


Fig. 7. Drag reducing effects of different systems under variable displacement. (a) 25 $^{\circ}$ C; (b) 90 $^{\circ}$ C.



 $\textbf{Fig. 8.} \ \ \textbf{Rheological properties of slickwater. (a) Steady-shear; (b) \ \ \textbf{Viscoelasticity.}$

reducing effect. As the displacement increases, the drag reduction rate gradually increases. After exceeding 50 L/min, the drag reducing effect starts to decline. The highest drag reduction rate is 76.85%. At 30 L/min, the temperature-resistant slickwater shows the highest drag reduction rate of 73.53%. However, when the temperature is increased to 90 °C, the spatial structure becomes unstable, leading to a significant reduction in drag reducing effect for both DRA and HPAM, with final drag reduction rates of less than 60%. In contrast, the temperature-resistant slickwater exhibits a notable persistence in achieving a relatively high drag reduction rate, approximately 70%, even at 90 °C. This result can be attributed to the maintenance of a relatively complete spatial structure of the temperature-resistant drag reducing agent PDRA, in combination with the drainage aid and anti-expansion agent, which synergistically enhances the temperature resistance of the slickwater.

3.3.2. Rheology property

The variable shear viscosity of the temperature-resistant slick-water is presented in Fig. 8(a). As the shear rate increases in 10 min, shear thinning behavior is observed, and the viscosity continues to decrease slowly. The results indicate that the high viscosity at low shear rates is due to slow conformational changes of the polymer molecular chains. Under static conditions, the polymer molecular

chains undergo random stretching and interactions, which are disrupted as the shear rate increases. However, as the shear rate continues to increase, further degradation of macromolecules becomes difficult, leading to an insignificant decrease in viscosity relative to the shear rate (Yang et al., 2019). At a shear rate of $170 \, \mathrm{s}^{-1}$, the viscosity of the temperature-resistant slickwater still maintains $20 \, \mathrm{mPa}$ s.

The storage modulus G' and loss modulus G' of slickwater were measured and presented in Fig. 8(b). Both G' and G'' increase as the frequency increases, with a comparable rate of increase. G'' dominates at lower frequencies, indicating the liquid-like behavior of slickwater. On the other hand, G' dominates at higher frequencies, indicating its solid-like behavior (Liu et al., 2022). At this point, the polymers in the slickwater store a significant amount of energy due to their elastic properties, which can be fully released in turbulent flow to achieve drag reduction.

3.3.3. Temperature and shear resistance ability

The changes in the drag reduction rate at different temperatures were presented in Fig. 9(a) and (b). The results indicate that the drag reduction rate gradually decreases with an increase in temperature, with no significant difference between 25 and 50 $^{\circ}$ C. The initial drag reduction rate decreases by 3.53% when the

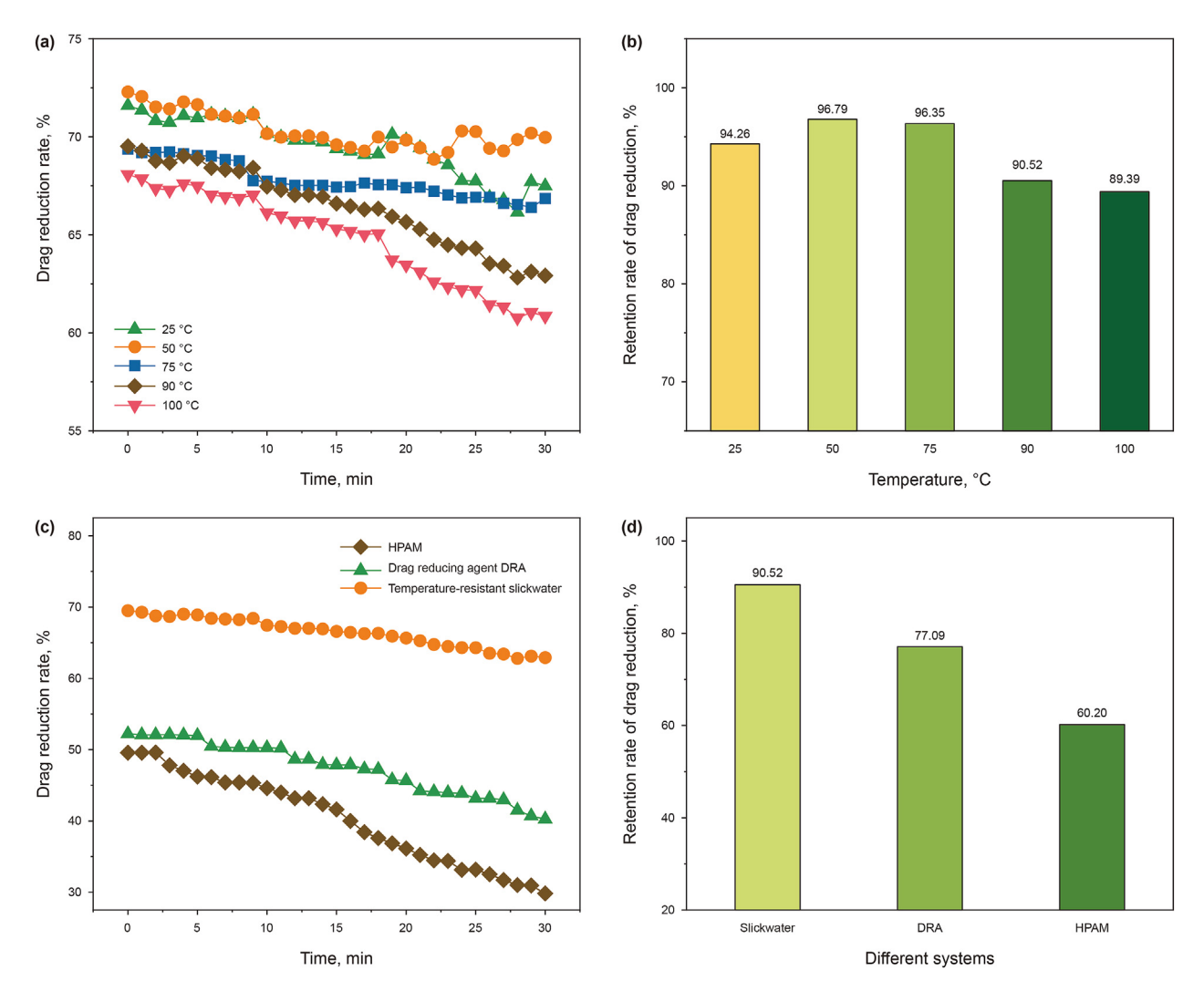
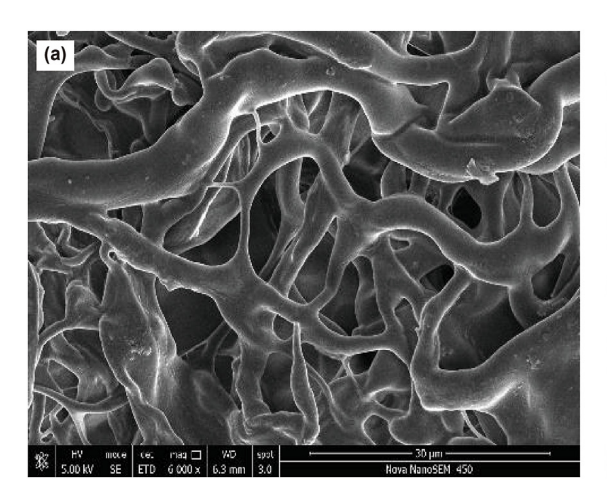


Fig. 9. (a) Variation of drag reduction rate of slickwater at different temperatures. (b) Retention rate of drag reduction of slickwater at different temperatures. (c) Variations of drag reduction rates of different systems at 90 °C. (d) Retention rates of drag reduction of different systems at 90 °C.



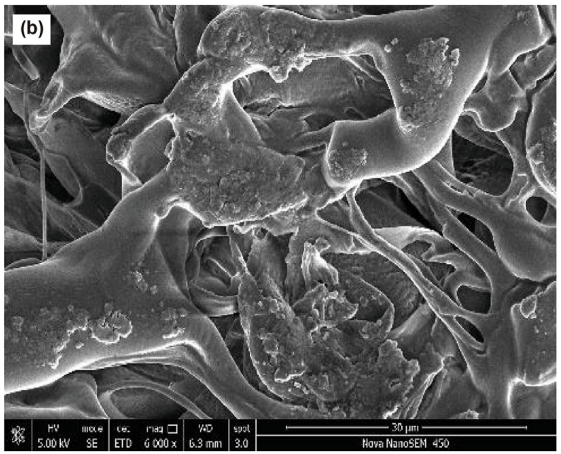


Fig. 10. Microscopic morphologies of temperature-resistant slickwater. (a) 25 °C; (b) 90 °C.

temperature is increased from 25 to 100 °C, indicating good temperature resistance of slickwater. After continuous shear for 30 min, the retention rate of drag reduction at 75 °C is 96.35%. However, when the temperature reaches 90 °C, the retention rate of drag reduction decreases to 90.52%. This is due to the breakage of some polymer molecular chains at high shear rates and the reduction of intermolecular hydrogen bonding. In either case, the spatial structure of the polymer becomes loose, which affects the energy storage and the drag reduction effect of slickwater.

Fig. 9(c) presents drag reduction rate variation curves with time for different systems at 90 °C. HPAM and drag reducing agent DRA exhibit poor drag reduction effect under high temperatures and shear rates, with the rate decreasing from 49.57% to 29.84% and from 52.22% to 40.25%, respectively. In addition, the drag reduction rate of slickwater decreases only from 69.51% to 62.92%, indicating its excellent temperature and shear resistance ability.

Microscopic morphologies of the temperature-resistant slickwater at different temperatures are depicted in Fig. 10. These images demonstrate that polymer network structure in slickwater aggregates and forms the "dendritic" connection. At 25 $^{\circ}$ C, slickwater not only accumulates in the polymer network structure, but also overlaps and attaches to the surface of the network structure. As the temperature rises to 90 $^{\circ}$ C, the polymer network structure of slickwater is partly fractured and crimped, but still maintains relatively dense, ensuring high drag reduction efficiency at elevated temperatures.

3.3.4. Core damage property

Fracturing fluids can inevitably disturb the original dynamic equilibrium of the formation (Fu et al., 2020; Zhang et al., 2019; Xu et al., 2016). Therefore, the degree of core damage caused by slickwater is a significant factor in determining its effectiveness. Upon injection of temperature-resistant slickwater into the core, there was a slight reduction in permeability from 2.17 to 2.05 mD, indicating some degree of core damage. The damage rate of the temperature-resistant slickwater was 5.53%, which increased slightly with the decrease in permeability, but remained at a low level.

4. Conclusions

In this work, a temperature-resistant polymeric drag reducing agent PDRA was synthesized using the solution polymerization method, and a temperature-resistant slickwater system was formulated with a composition of 0.2 wt% PDRA, 0.05 wt% drainage

aid NPEP and 0.5 wt% anti-expansion agent PDM. The performance of the slickwater system was systematically evaluated, including its drag reduction ability, rheology properties, temperature and shear resistance ability, and core damage property. The results demonstrate that the temperature-resistant slickwater exhibits excellent drag reduction ability at high temperatures, as well as good temperature and shear resistance and rheological properties. Additionally, the core damage rate is at a low level. All the performance evaluations meet the standards of the water-based fracturing fluid. This work represents a novel approach to enhancing the stability of slickwater, which could be particularly valuable for unconventional reservoirs.

CRediT authorship contribution statement

Ming-Wei Zhao: Writing — original draft, Writing — review & editing. Zhen-Feng Ma: Investigation, Writing — original draft. Cai-Li Dai: Resources, Supervision, Writing — review & editing. Wei Wu: Resources. Yong-Quan Sun: Resources. Xu-Guang Song: Methodology, Software. Yun-Long Cheng: Methodology, Software. Xiang-Yu Wang: Methodology, Software.

Declaration of competing interest

The authors declare that they have no known competing financial interests or personal relationships that could have appeared to influence the work reported in this paper.

Acknowledgements

The work was supported by the National Natural Science Foundation of China (Nos. 52222403, 52074333, 52120105007), and Taishan Scholar Young Expert (No. tsqn202211079).

References

Abdollahi, Z., Frounchi, M., Dadbin, S., 2011. Synthesis, characterization and comparison of PAM, cationic PDMC and P(AM-co-DMC) based on solution polymerization. J. Ind. Eng. Chem. 17 (3), 580–586. https://doi.org/10.1016/j.jiec.2010.10.030.

Argyropoulos, C.D., Markatos, N.C., 2015. Recent advances on the numerical modelling of turbulent flows. Appl. Math. Model. 39 (2), 693–732. https://doi.org/10.1016/j.apm.2014.07.001.

Asidin, M.A., Suali, E., Jusnukin, T., Lahin, F.A., 2019. Review on the applications and developments of drag reducing polymer in turbulent pipe flow. Chin. J. Chem. Eng. 27 (8), 1921–1932. https://doi.org/10.1016/j.cjche.2019.03.003.

Eng. 27 (8), 1921–1932. https://doi.org/10.1016/j.cjche.2019.03.003.
Bai, H., Zhou, F., Zhang, M., et al., 2021. Optimization and friction reduction study of a new type of viscoelastic slickwater system. J. Mol. Liq. 344, 117876. https://

doi.org/10.1016/j.molliq.2021.117876.

- Barati, R., Liang, J., 2014. A review of fracturing fluid systems used for hydraulic fracturing of oil and gas wells. J. Appl. Polym. Sci. 131 (16). https://doi.org/ 10.1002/app.40735.
- Birdsell, D.T., Rajaram, H., Dempsey, D., Viswanathan, H.S., 2015. Hydraulic fracturing fluid migration in the subsurface: a review and expanded modeling results. Water Resour. Res. 51 (9), 7159–7188. https://doi.org/10.1002/2015WR017810.
- Chen, R., Sun, K., Zhang, Q., et al., 2019. Sequential solution polymerization of poly(3,4-ethylenedioxythiophene) using V₂O₅ as oxidant for flexible touch sensors. iScience 12, 66–75. https://doi.org/10.1016/j.isci.2019.01.003.
- Deng, Z., Liu, M., Qin, J., et al., 2022. Mechanism study of water control and oil recovery improvement by polymer gels based on nuclear magnetic resonance. J. Pet. Sci. Eng. 209, 109881. https://doi.org/10.1016/j.petrol.2021.109881.
- Elhaei, R., Kharrat, R., Madani, M., 2021. Stability, flocculation, and rheological behavior of silica suspension-augmented polyacrylamide and the possibility to improve polymer flooding functionality. J. Mol. Liq. 322, 114572. https://doi.org/ 10.1016/j.molliq.2020.114572.
- Fu, L., Liao, K., Ge, J., et al., 2020. Study on the damage and control method of fracturing fluid to tight reservoir matrix. J. Nat. Gas Sci. Eng. 82, 103464. https:// doi.org/10.1016/j.jngse.2020.103464.
- Funkhouser, G.P., Holtsclaw, J., Blevins, J.J., 2010. Hydraulic fracturing under extreme HPHT conditions: successful application of a new synthetic fluid in south Texas gas wells. In: SPE Deep Gas Conference and Exhibition. https://doi.org/10.2118/132173-MS.
- Guo, J., Li, Y., Wang, S., 2018. Adsorption damage and control measures of slick-water fracturing fluid in shale reservoirs. Petrol. Explor. Dev. 45 (2), 336–342. https://doi.org/10.1016/S1876-3804(18)30037-5.
- Gupta, D.V., Carman, P.S., 2011. Associative polymer system extends the temperature range of surfactant gel frac fluids. In: SPE International Symposium on Oilfield Chemistry. https://doi.org/10.2118/141260-MS.
- Hu, X., Wu, K., Li, G., Tang, J., Shen, Z., 2018. Effect of proppant addition schedule on the proppant distribution in a straight fracture for slickwater treatment. J. Pet. Sci. Eng. 167, 110–119. https://doi.org/10.1016/j.petrol.2018.03.081.
- Karami, H.R., Mowla, D., 2012. Investigation of the effects of various parameters on pressure drop reduction in crude oil pipelines by drag reducing agents. J. Nonnewton. Fluid. Mech. 177–178, 37–45. https://doi.org/10.1016/ j.innfm.2012.04.001.
- Korlepara, N.K., Patel, N., Dilley, C., et al., 2022. Understanding effect of fluid salinity on polymeric drag reduction in turbulent flows of slickwater fluids. J. Pet. Sci. Eng. 216, 110747. https://doi.org/10.1016/j.petrol.2022.110747.
- Li, Q., Pu, W., Wang, Y., Zhao, T., 2013. Synthesis and assessment of a novel AM-co-AMPS polymer for enhanced oil recovery (EOR). In: 2013 International Conference on Computational and Information Sciences, pp. 997–1000. https://doi.org/10.1109/ICCIS.2013.267.
- Li, Q., Xing, H., Liu, J., Liu, X., 2015. A review on hydraulic fracturing of unconventional reservoir. Petroleum 1 (1), 8–15. https://doi.org/10.1016/i.petlm.2015.03.008.
- Lin, J., Wu, X., Zheng, C., et al., 2014. Synthesis and properties of epoxypolyurethane/silica nanocomposites by a novel sol method and in-situ solution polymerization route. Appl. Surf. Sci. 303, 67–75. https://doi.org/10.1016/ j.apsusc.2014.02.075.
- Liu, S., Zhao, M., Wu, Y., et al., 2022. Development and performance evaluation of a novel silica nanoparticle-reinforced CO₂-sensitive fracturing fluid with high temperature and shear resistance ability. Energy Fuel. 36 (13), 7177–7185. https://doi.org/10.1021/acs.energyfuels.2c01056.
- Montgomery, C., 2013. Fracturing fluids. In: ISRM International Conference for Effective and Sustainable Hydraulic Fracturing. https://doi.org/10.5772/56192.

- Nguyen, T.C., Romero, B., Vinson, E., Wiggins, H., 2018. Effect of salt on the performance of drag reducers in slickwater fracturing fluids. J. Pet. Sci. Eng. 163, 590–599. https://doi.org/10.1016/j.petrol.2018.01.006.
- Osiptsov, A.A., 2017. Fluid mechanics of hydraulic fracturing: a review. J. Pet. Sci. Eng. 156, 513–535. https://doi.org/10.1016/j.petrol.2017.05.019.
- Patel, P.S., Robart, C.J., Ruegamer, M., Yang, A., 2014. Analysis of US hydraulic fracturing fluid system and proppant trends. In: SPE Hydraulic Fracturing Technology Conference. https://doi.org/10.2118/168645-MS.
- Pawar, M., Kadam, A., Yemul, O., Thamke, V., Kodam, K., 2016. Biodegradable bio-epoxy resins based on epoxidized natural oil (cottonseed & algae) cured with citric and tartaric acids through solution polymerization: a renewable approach. Ind. Crops Prod. 89, 434–447. https://doi.org/10.1016/j.indcrop.2016.05.025.
- Sheng, J.J., 2017. Critical review of field EOR projects in shale and tight reservoirs. J. Pet. Sci. Eng. 159, 654–665. https://doi.org/10.1016/j.petrol.2017.09.022.
- Shi, J., Biegler, L.T., Hamdan, I., Wassick, J., 2016. Optimization of grade transitions in polyethylene solution polymerization process under uncertainty. Comput. Chem. Eng. 95, 260–279. https://doi.org/10.1016/j.compchemeng.2016.08.002.
- Varnaseri, M., Peyghambarzadeh, S.M., 2020. The effect of polyacrylamide drag reducing agent on friction factor and heat transfer coefficient in laminar, transition and turbulent flow regimes in circular pipes with different diameters. Int. J. Heat Mass Tran. 154, 119815. https://doi.org/10.1016/j.ijjheatmasstransfer.2020.119815.
- Wang, H., Zhou, D., Xu, J., et al., 2021. An optimal design algorithm for proppant placement in slickwater fracturing. In: Abu Dhabi International Petroleum Exhibition & Conference. https://doi.org/10.2118/207617-MS.
- Wang, J., Zhou, F., Bai, H., Li, Y., Yang, H., 2020a. A comprehensive method to evaluate the viscous slickwater as fracturing fluids for hydraulic fracturing applications. J. Pet. Sci. Eng. 193, 107359. https://doi.org/10.1016/j.petrol.2020.107359.
- Wang, J., Zhou, F., Bai, H., et al., 2020b. A new approach to study the friction-reduction characteristics of viscous/conventional slickwater in simulated pipelines and fractures. J. Nat. Gas Sci. Eng. 83, 103620. https://doi.org/10.1016/j.ingse.2020.103620.
- Wang, J., Guo, P., Jiang, H., Zhou, F., 2022. A novel multifunction fracturing fluid compounding of nano-emulsion and viscous slickwater for unconventional gas and oil. Arab. J. Chem. 15 (5), 103749. https://doi.org/10.1016/ j.arabjc.2022.103749.
- Wu, Z., Cui, C., Jia, P., Wang, Z., Sui, Y., 2022. Advances and challenges in hydraulic fracturing of tight reservoirs: a critical review. Energy Geosci. 3 (4), 427–435. https://doi.org/10.1016/j.engeos.2021.08.002.
- Xu, K., Lu, Y., Chang, J., Lu, X., Wang, P., 2022. Research and performance analysis of 245 °C Ultra-high temperature fracturing liquid. In: Lin, J.E. (Ed.), Proceedings of the International Field Exploration and Development Conference 2021, pp. 4536–4541. https://doi.org/10.1007/978-981-19-2149-0_423.
- Xu, Z., Li, Z., Wang, C., Adenutsi, C.D., 2016. Experimental study on microscopic formation damage of low permeability reservoir caused by HPG fracturing fluid. J. Nat. Gas Sci. Eng. 36, 486–495. https://doi.org/10.1016/j.jngse.2016.10.063.
- Yang, B., Zhao, J., Mao, J., et al., 2019. Review of friction reducers used in slickwater fracturing fluids for shale gas reservoirs. J. Nat. Gas Sci. Eng. 62, 302–313. https://doi.org/10.1016/j.jngse.2018.12.016.
- Yang, D., Peng, X., Peng, Q., et al., 2022. Probing the interfacial forces and surface interaction mechanisms in petroleum production processes. Engineering 18, 49–61. https://doi.org/10.1016/j.eng.2022.06.012.
- Zhang, L., Zhou, F., Zhang, S., et al., 2019. Evaluation of permeability damage caused by drilling and fracturing fluids in tight low permeability sandstone reservoirs. J. Pet. Sci. Eng. 175, 1122—1135. https://doi.org/10.1016/j.petrol.2019.01.031.